Received: 23 October 2019 | Revised: 28 December 2019 | Accepted: 6 January 2020

DOI: 10.1111/pce.13717

ORIGINAL ARTICLE

Plant, Cell & Environment WILEY

A point mutation in *LTT1* enhances cold tolerance at the booting stage in rice

Yufang Xu[1,2] | Ruci Wang[1] | Yueming Wang[1] | Li Zhang[1,2] | Shanguo Yao[1]

[1]State Key Laboratory of Plant Genomics, Institute of Genetics and Developmental Biology, The Innovative Academy of Seed Design, Chinese Academy of Sciences, Beijing, China

[2]Genome Biology Center, University of Chinese Academy of Sciences, Beijing, China

Correspondence
Shanguo Yao, State Key Laboratory of Plant Genomics, Institute of Genetics and Developmental Biology, Chinese Academy of Sciences, No.1 West Beichen Road, Chaoyang District, Beijing 100101, China.
Email: sgyao@genetics.ac.cn

Funding information
the National Key Research and Development Program of China, Grant/Award Number: 2016YFD0101801; the State Key Laboratory of Plant Genomics, Grant/Award Number: SKLPG2011B0403

Abstract

The cold tolerance of rice at the booting stage is a main factor determining sustainability and regional adaptability. However, relatively few cold tolerance genes have been identified that can be effectively used in breeding programmes. Here, we show that a point mutation in the *low-temperature tolerance 1* (*LTT1*) gene improves cold tolerance by maintaining tapetum degradation and pollen development, by activation of systems that metabolize reactive oxygen species (ROS). Cold-induced ROS accumulation is therefore prevented in the anthers of the *ltt1* mutants allowing correct development. In contrast, exposure to cold stress dramatically increases ROS accumulation in the wild type anthers, together with the expression of genes encoding proteins associated with programmed cell death and with the accelerated degradation of the tapetum that ultimately leads to pollen abortion. These results demonstrate that appropriate ROS management is critical for the cold tolerance of rice at the booting stage. Hence, the *ltt1* mutation can significantly improve the seed setting ability of cold-sensitive rice varieties under low-temperature stress conditions, with little yield penalty under optimal temperature conditions. This study highlights the importance of a valuable genetic resource that may be applied in rice breeding programmes to enhance cold tolerance.

KEYWORDS

booting stage, cold tolerance, *LTT1*, rice, ROS acclimation

1 | INTRODUCTION

Rice is an important model plant and food crop originating in tropical and subtropical regions and is more sensitive to low temperature than other cereal crops (Gross & Zhao, 2014; Zhang, Chen, Wang, Hong, & Wang, 2014). Low temperature affects adversely the development of rice plants from germination to grain filling. Especially, cold stress at the booting stage often causes abnormal hypertrophy or dissolution of tapetal cells, interferes with the nutrition supply from anther walls to young microspore, and leads to pollen abortion and male sterility (Sharma & Nayyar, 2016). Because low temperature has been a major limiting factor for rice productivity and geographical distribution, much effort has been put on discovering cold-tolerant genes. Over the past decades, multiple cold-tolerant quantitative trait loci (QTLs) or genes have been roughly mapped, and some of them have been cloned. For example, *qLTG3-1* is identified as a major QTL for low-temperature germinability (Fujino et al., 2008), and *LTG1*, *COLD1*, *bZIP73*, *qBSR10*, and *HAN1* are responsible for cold tolerance at the seedling stage (Liu et al., 2018; Lu et al., 2014; Ma et al., 2015; Mao et al., 2019; Xiao et al., 2018). In fact, both germination and seedling growth could be managed in a controlled environment, whereas rice plants at the booting stage are completely under natural field conditions and could not be artificially protected. Therefore, enhancing cold tolerance at the booting stage is particularly important for rice

breeding in high latitudes. However, due to the lack of precise phenotype evaluation system, few reliable genes/QTLs related to this trait have thus far been identified and functionally characterized in rice. So far, only three genes of *Ctb1*, *bZIP73*, and *CTB4a* are reported to be involved in cold tolerance at the booting stage. However, the function of *Ctb1* in the booting stage cold tolerance remains elusive because conclusive genetic evidence still remains blank (Saito, Hayano-Saito, Kuroki, & Sato, 2010). Although natural variation in *CTB4a* appears to enhance the tolerance of rice to cold stress (Zhang et al., 2017), some of the varieties with the most effective haplotype (Hap1), such as DAOHUAXIANG and DONGNONG428, are highly sensitive to cold stress during the booting stage. Similarly, *bZIP73* was identified as a QTL for seedling chilling tolerance (Liu et al., 2018), and the function of this gene on cold tolerance at the booting stage could only be observed in transgenic lines (Liu et al., 2019). In view of the severe damage of booting stage cold stress on rice yield and the functional uncertainties of the currently reported cold tolerance genes, there is an urgent need to provide effective cold tolerant genetic resources for traditional breeding.

The direct consequence of low-temperature stress at the booting stage is the decrease in seed setting and thus reduction in the final grain yield. Therefore, the spikelet fertility is regarded as the key index to evaluate the booting stage cold tolerance (Zhang et al., 2014), which is largely determined by a series of key processes including tapetum degradation, anther dehiscence, and pollen fertilization. As the innermost cell layer of the anther, the tapetum connects the male gametophyte and sporophyte and secretes callose and provides nutrients during pollen development, which are crucial in the release of microspores from tetrads, microspore development, and pollen exine formation. Many studies have shown that the timely degradation of tapetum, a genetically controlled process of programmed cell death (PCD), is the most important factor to ensure the normal development of pollen and thus seed setting (Li et al., 2006; Zhang et al., 2008). Normally, the tapetal PCD process is initiated at the microsporocyte meiosis stage, featured by vacuolated and shrunken cytoplasm, swelling endoplasmic reticulum and nuclear DNA fragmentation, and degradation of the tapetal cells, which is almost completed until the first mitotic division of microspore. Abnormal tapetal PCD, regardless if premature or retarded, would lead to male sterility (Sharma & Nayyar, 2016).

The timely initiation of tapetal PCD during microspore development is found to be largely affected by dynamic changes of the endogenous level of reactive oxygen species (ROS; Hu et al., 2011; Ko et al., 2017; Xie, Wan, Li, & Zhang, 2014; Yu, Feng, Xie, Li, & Zhang, 2017), which are key signalling molecules involved in various biological processes and stress responses (Mittler, 2017). Relevant researches have unveiled that the cellular ROS level is very sensitive to temperature changes, and maintaining ROS homeostasis associates intimately with the adaptation to extreme temperature in rice (Baxter, Mittler, & Suzuki, 2014; Zhang et al., 2016). Under cold stress, the intracellular ROS level increases dramatically, which would activate rapidly the antioxidant defence systems by upregulating the expression of genes involved in ROS scavenging (Dreyer & Dietz, 2018). On the other hand, increased ROS level would trigger multiple regulatory networks such as MAPK cascades and MYB- and WRKY-mediated transcriptional regulation to activate cold-responsive signalling pathways (Cheng et al., 2007; Peres, Basu, Ramegowda, Braga, & Pereira, 2016; Tao et al., 2011; Xie, Kato, & Imai, 2012; Zhang et al., 2014; Zhang et al., 2016). When plants continue to suffer from severe cold stress, the intracellular ROS would accumulate excessively, leading to a series of cytotoxic effects such as cell death, lipid peroxidation, photosynthetic rate reduction, growth retardation, and even seedling death or spikelet sterility (Liu et al., 2018; Sato, Masuta, Saito, Murayama, & Ozawa, 2011; Suzuki et al., 2015; Tovuu et al., 2016). Generally, over accumulation of ROS in the anther during microspore development would cause premature tapetal PCD (Luo et al., 2013; Zheng et al., 2019), whereas reduced ROS content would delay the PCD process in the tapetum (Yi et al., 2016). However, the molecular mechanism underlying how cold stress influences tapetal PCD by altering the steady-state level of ROS in the anthers remains unclear.

In this study, we report that a point mutation in *LTT1* endows the plants with much increased seed setting under low-temperature stress conditions. We provide evidence that the mutation results in plants with re-established ROS homeostasis at higher endogenous levels and acclimation of the mutant plants to oxidative stress enables them to cope well with the coming cold stress and maintain normal anther development under the stress conditions. Although we are unable to uncover at present the molecular mechanism of *LTT1* in regulating low-temperature tolerance at the booting stage, the performance of the NIL-*ltt1* under the background of the major cultivar DAOHUAXIANG (DHX) clearly demonstrates that the mutation is of great potential in practical cold tolerance breeding in rice.

2 | MATERIALS AND METHODS

2.1 | Plant materials and growth conditions

The *ltt1* mutant was screened from sodium azide-mutagenized M_2 population of ZY66 (*japonica*). The mapping population was generated by crossing *ltt1* with KY131 (*japonica*). All the materials used in this study were cultivated in the experimental fields of the Institute of Genetics and Developmental Biology in Changping (40.2°N/116.2°E), Beijing during the summer or Lingshui (18.5°N, 110.0°E), Hainan province during the winter.

To eliminate the influence of differential heading date on agronomic trait evaluation, DHX, the major cultivar of Wuchang, Heilongiang province (44.9°N/127.2°E), was first crossed with LJ31 (*japonica*), and NIL-*Dg* (BC_4F_4) was developed by repeated backcrossing with DHX. The *ltt1* mutation was then introduced into the background of NIL-*Dg* to construct NIL-*Dgl* (BC_4F_4). Makers used for selection were listed in Table S1. Performance of the NIL-*Dgl* was evaluated under the natural conditions in Beijing, with planting densities of 20 × 20 cm (ID1), 17 × 16 cm (ID2), and 15 × 12 cm (ID3). To exclude background noise, three independent homozygous plants with or without the *ltt1* mutation were selected from the same genetic population for phenotypic comparison.

2.2 | Stress tolerance assay

To observe booting stage cold resistance under natural conditions, plants were grown in Lingshui in January and February, the winter season with an average daily temperature generally below 20°C. To ensure that all the materials could be exposed to low-temperature stress at the same developmental stage, we adopted a batch sowing approach by sowing the seeds once a week from November 1 to December 12. The microsporocyte meiosis stage was judged as the pulvinus of the flag leaf, and the penultimate leaf was overlapped.

To evaluate booting stage cold tolerance under controlled conditions, germinating seeds were sowed every 5 days from April 16 to May 10, and the seedlings of four-leaf stage were transplanted into pots (25 × 25 × 35 cm). Four plants were grown in each pot and cultured under natural conditions in Beijing. The tillers at the microsporocyte meiosis stage were tagged and treated with 17°C for 7 days in the phytotron (PERCIVAL, USA), with 14-hr light /10-hr dark, 65–70% relative humidity, and 600 $\mu molm^{-2}\ s^{-1}$ photon flux density, and then recovered under normal growth conditions until seed maturation.

To evaluate seedling chilling tolerance, two-leaf-stage seedlings grown under normal conditions were treated with 4°C for 7 days in the phytotron (SANYO, Japan), with 14-hr light/10-hr dark, 60–70% relative humidity, and 200 $\mu molm^{-2}\ s^{-1}$ photon flux density. For oxidative stress assay, water-cultured 30-day-old seedlings were transferred to 80-mM H_2O_2-containing medium for 10 days in the phytotron (SANYO, Japan), with 14-hr light (28°C)/10-hr dark (25°C), 60–70% relative humidity, and 200 $\mu molm^{-2}\ s^{-1}$ photon flux density. After cold or oxidative stress treatment, seedlings were recovered under normal conditions for 7 days in the phytotron (SANYO, Japan), with 14-hr light (28°C)/10-hr dark (25°C), 60–70% relative humidity, and 200 $\mu molm^{-2}\ s^{-1}$ photon flux density. The survival rate was calculated as the ratio of the number of seedlings with fully opened green leaves to the total number of treated seedlings. For low-temperature germinability assay, healthy seeds were surface sterilized with 3% sodium hypochlorite for 30 min and then soaked with distilled water under 30°C and 15°C. The germination rate was investigated every 3 days.

2.3 | Microscopy

Paraffin sectioning and scanning electron microscopic observation were performed according to the method previously described (Wang et al., 2017b). Anthers were sampled at different developmental stages as defined previously (Zhang, Luo, & Zhu, 2011). The embryo sac was observed according to Shi et al. (2018), and trypan blue staining was performed according to Chen et al. (2016). Pollen viability was analysed by 1% I_2/KI staining.

2.4 | Terminal deoxynucleotidyl transferase-mediated dUTP nick end labelling assay

Transverse sections of leaves and anthers with and without cold treatment were prepared by the same way as that of the light microscopy. According to the manufacturer's instruction, the sections were subjected to the terminal deoxynucleotidyl transferase-mediated dUTP nick end labelling (TUNEL) assay using the DeadEnd™ Fluorometric TUNEL System (Promega). The green fluorescence of fluorescein (TUNEL signal) and red fluorescence of propidium iodide were analysed with the excitation wavelength of 488 nm and the detection wavelength of 520 and 620 nm, respectively, under the laser scanning confocal microscopy (Leica TCS SP5).

2.5 | Detection of ROS accumulation

Newly opened leaves were sampled from plants at 14, 30, 50, and 80 days after sowing, and H_2O_2 quantification was performed according to the way previously described (Garg, Jaiswal, Misra, Tripathi, & Prasad, 2012). The accumulation of H_2O_2 was detected by 0.1% 3,3'-diaminobenzidine staining, and superoxide anion was visualized by nitroblue tetrazolium (NBT) staining (Hu et al., 2011). 2',7'-dichlorodihydrofluorescein diacetate (H_2DCF-DA) staining was carried out according to the method by Xie et al. (2014), and relative fluorescence intensity was quantified by the software integrated in the Leica TCS SP5 microsystem.

2.6 | Measurement of superoxide dismutase and peroxidases activity

A 0.5 g of leaves were collected from 60-day-old plants under natural conditions, and superoxide dismutase (SOD) and peroxidases activities were measured according to the method described by Ouyang et al. (2010)

2.7 | Plasmid construction and transformation

For complementation test, the 5,561-bp genomic DNA containing the entire open reading frame (ORF), 2561-bp upstream sequence, and 489-bp downstream sequence of *Os10g34110* was amplified from *ltt1* and ligated into the binary vector pZH2B. For overexpression assay, the entire ORF of *Os10g34110* was amplified from *ltt1*, and the 5,561-bp genomic DNA used for complementation test was amplified from *ltt1* and wild type (WT) and was ligated into the binary vector pZH2Bi driven by the ubiquitin promoter. To create *Os10g34110* knockdown plants, the hairpin sequence with two ~300-bp cDNA-inverted repeats was inserted into pZH2Bi. After confirming the sequence, all of the resultant constructs were introduced into *Agrobacterium tumefaciens* strain EHA105 and transferred into recipient materials by the *Agrobacterium*-mediated method. For *Os10g34110* knockout assay, plasmid construction and plant transformation were all performed by BIOGLE GeneTech (Hangzhou, China). The primers used for vector construction are listed in Table S1.

2.8 | Quantitative real-time RT-PCR

To detect the expression of *Rbohs* and tapetal PCD genes, the anthers at Stage 9 were sampled from plants under natural and cold-stressed (17°C, 7 days) conditions, respectively. For expression analysis of *AOXs* and genes involved in ROS scavenging, newly opened leaves were collected from 50-day-old plants under natural conditions. Total RNA was isolated using a RNAiso Plus Kit (TaKaRa), and 1-μg RNA was reverse transcribed into first-strand cDNA according to the protocol (Promega) after digestion with ribonuclease-free deoxyribonuclease I (Fermentas). The qRT-PCR assay was carried out using SYBR Green I Master reagent and a LightCycler Nano system (Roche). The *Actin1* gene was used as an endogenous control for normalization. The primers used are listed in Table S1.

2.9 | Accession numbers

The sequence data in this paper can be found in the European Molecular Biology Laboratory /GenBank data libraries under the following accession numbers: *OsActin1*, *Os03g50885*; *OsAGO2*, *Os04g52540*; *OsHXK1*, *Os07g26540*; *OsUDT1*, *Os07g36460*; *OsTIP2*, *Os01g18870*; *OsTDR1*, *Os02g02820*; *OsEAT1*, *Os04g51070*; *OsMYB80/OsMYB103*, *Os04g39470*; *OsTGA10*, *Os09g31390*; *OsPTC1*, *Os09g27620*; *OsMADS3*, *Os01g10504*; *OsDTC1*, *Os07g35610*; *OsRboh1*, *Os01g25820*; *OsRboh2*, *Os01g53294*; *OsRboh3*, *Os01g61880*; *OsRboh4*, *Os05g38980*; *OsRboh5*, *Os05g45210*; *OsRboh6*, *Os08g35210*; *OsRboh7*, *Os09g26660*; *OsRboh8*, *Os11g33120*; *OsRboh9*, *Os12g35610*; *APX1*, *Os03g17690*; *APX3*, *Os04g14680*; *APX7*, *Os04g35520*; *SODA1*, *Os05g25850*; *SODB*, *Os06g05110*; *SODCC2*, *Os07g46990*; *CATA*, *Os02g02400*; *CATB*, *Os06g51150*; *CATC*, *Os03g03910*; *GPX1*, *Os04g46960*; *GPX2*, *Os03g24380*; *GPX3*, *Os02g44500*; *AOX1a*, *Os04g51150*; *AOX1b*, *Os04g51160*; *AOX1c*, *Os02g47200*.

3 | RESULTS

3.1 | *ltt1* is identified as a cold-tolerant mutant

By screening a NaN3-mutagenized M_2 library in the background of ZY66, a *japonica* cultivar exhibiting extreme sensitivity to low-temperature stress, we identified a mutant with high seed setting under cold stress conditions (Figure 1a–c) and then named it as *low-temperature tolerance 1* (*ltt1*). Through planting of the selfing progenies, we found that the mutant showed stable high seed setting rate of 89.5%, 71.9%, and 84.9% in the consecutive 3 years of 2017, 2018, and 2019 under natural cold stress conditions in Lingshui, Hainan province, in contrast to that of 44.4%, 10.0%, and 43.5% of the WT, respectively (Figure S1). We further confirmed the cold tolerant phenotype of *ltt1* by subjecting the mutant and WT to low-temperature stress in phytotron during the microsporocyte meiosis stage. After 7 days of treatment at 17°C, the seed setting rate of the WT plants was no more than 10%, whereas that of *ltt1* could reach to about 70% (Figure 1d–f). No difference could be observed for the seed setting between *ltt1* and WT under normal conditions (Figure S2a,f).

To test whether *LTT1* also plays a role in cold tolerance at other growth stages, we carried out low-temperature treatment for germinating seeds and 15-day-old seedlings. No obvious difference was detected for germinability between *ltt1* and WT under 15°C treatment (Figure S3a,b). After treating the seedlings for 7 days at 4°C, we found that *ltt1* showed a survival rate of approximately twice that of the WT (82% vs. 41%; Figure S3c,d). These observations indicate that *LTT1* functions in cold tolerance at the booting stage and chilling tolerance at the seedling stage.

To understand the low-temperature-induced difference of spikelet fertility between *ltt1* and WT, we compared the morphology of reproductive organs in *ltt1* with WT under normal and cold treatment conditions. We frequently observed distorted and deformed anthers in the WT plants under cold stress, whereas *ltt1* showed little changes in anther morphology (Figures 1g and S4a,b). Consequently, the pollen grains of the WT were shrivelled and sunk after cold stress, in contrast to those normally developed in the mutant (Figure 1h,i). We also observed the female organs under both environmental conditions and found no obvious morphological changes in the pistils of both *ltt1* and WT after low-temperature treatment (Figure S4c,d). These results demonstrate that *ltt1* could maintain relatively normal anther development and pollen vitality under cold stress, which is responsible for the high spikelet fertility.

When crossing the mutant with WT, we found that the F_1 plants showed intermediate phenotypes in overall traits including heading date, plant height, tiller number per plant, and low-temperature seed setting (Figures S2 and S5). And the resultant F_2 population segregated into three distinct phenotypes of 230 WT, 435 heterozygotes [*ltt1*(+/−)], and 199 homozygous [*ltt1*(−/−)], which fits exactly to a ratio of 1:2:1 ($\chi^2 = 2.27$; $0.5 > p > .1$), indicating the semi-dominant feature of *LTT1* for the mutant phenotype.

An intuitive phenotype of the *ltt1* mutant was the distinct lesion mimic in the leaf (Figure S2d). When growing to about four-leaf stage, the newly opened leaf and its lower leaf in *ltt1* gradually turned yellow from the tip, and reddish-brown spots then appeared and gradually enlarged and finally extended to the leaf body at the early tillering stage (Figure 2a). The lesion mimic phenotype was aggravated along with the vegetative growth and the increase of leaf age, with older leaves showing severe lesions and newly emerging leaves showing no lesions but are slightly yellow (Figure S2d). Very interestingly, the lesion mimic phenotype was hardly developed on the flag leaf formed during reproductive growth (Figure 2a).

3.2 | *ltt1* shows increased endogenous ROS level

The lesion mimic phenotype in the mutant indicates the occurrence of PCD process, which is usually accompanied by excessive production of ROS (Choudhury, Rivero, Blumwald, & Mittler, 2017; Mittler, 2017). Consistent with the phenotypic variations between *ltt1*(+/−) and *ltt1* (−/−) plants (Figure S2), we detected clear dosage effect of this mutation on the endogenous level of hydrogen peroxide (H_2O_2), and the

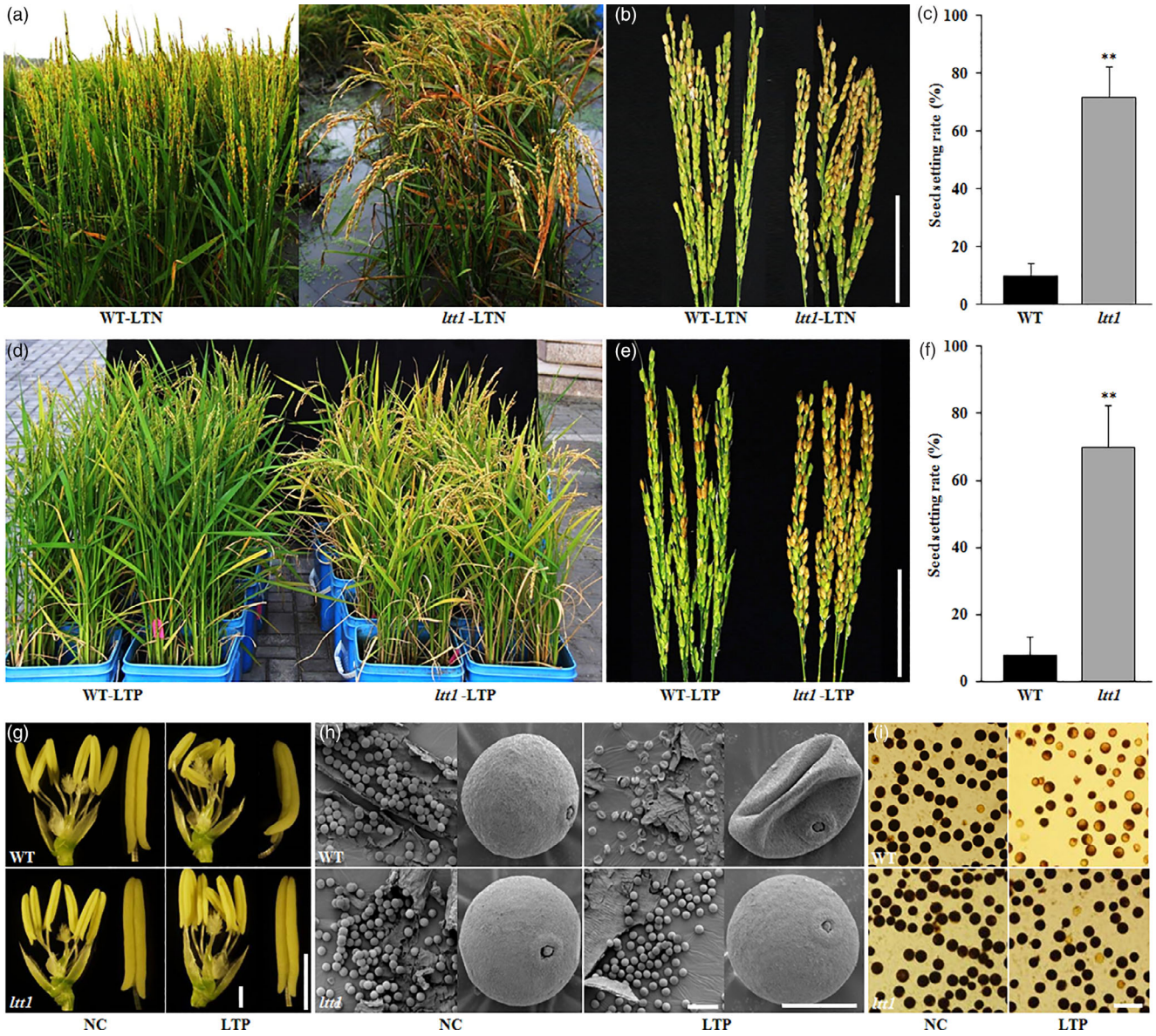

FIGURE 1 *ltt1* is a cold-tolerant mutant. (a–f) Cold tolerant phenotype of *ltt1* shown by population (a,d) and panicles (b,e). Bars = 5 cm. (c,f) Statistical analysis of seed setting under LTN (Lingshui, 2018) and LTP (Beijing, 2018), respectively. Data are means ± *SD* ($n = 20$). $^{**}p < .01$ (Student's *t*-test). (g,h) Morphology of anther (g) and pollen grain (h) under NC and LTP, respectively. Bars = 1 (g), 100 (left), and 20 μm (right; h). (i) Pollen fertility comparison. Pollen grains were stained with I_2-KI. Bar = 100 μm. LTN, low temperature under natural conditions; LTP, low temperature under phytotron conditions (17°C, 7 days); NC, normal conditions; WT, wild type

H_2O_2 content at various growth stages was closely linked to the severity of the lesion mimic phenotype (Figure 2a,b). We further performed 3,3′-diaminobenzidine and NBT staining to visualize the production of H_2O_2 and superoxide anion, respectively. The conspicuous staining in the leaves of *ltt1*(−/−) indicated the higher concentrations of H_2O_2 and superoxide anion compared with that in the WT, (Figure 2c). And H_2DCF-DA staining also revealed clearly that the content of ROS in the cells of the mutant was obviously higher than that of the WT (Figure 2d). Moreover, the leaves of *ltt1*(−/−) displayed densest dark blue spots after TB staining compared with that of WT or *ltt1*(+/−; Figure 2c), indicating the most severe membrane damage or cell death in the *ltt1*(−/−) plants. We also performed TUNEL assay to visualize directly the PCD signals. We observed strong TUNEL-positive signals in the leaves of *ltt1*, indicating the occurrence of intensive PCD in the mutant (Figure 2e). Taken together, all the above experiments demonstrate that the mutation in *LTT1* results in the increase of endogenous ROS content, leading to the formation of lesion mimic phenotype in the mutant.

3.3 | *ltt1* shows normal tapetal PCD under cold stress

Tapetal PCD occurring at the proper stage of microspore development is crucial for normal pollen formation, and ROS could act as a

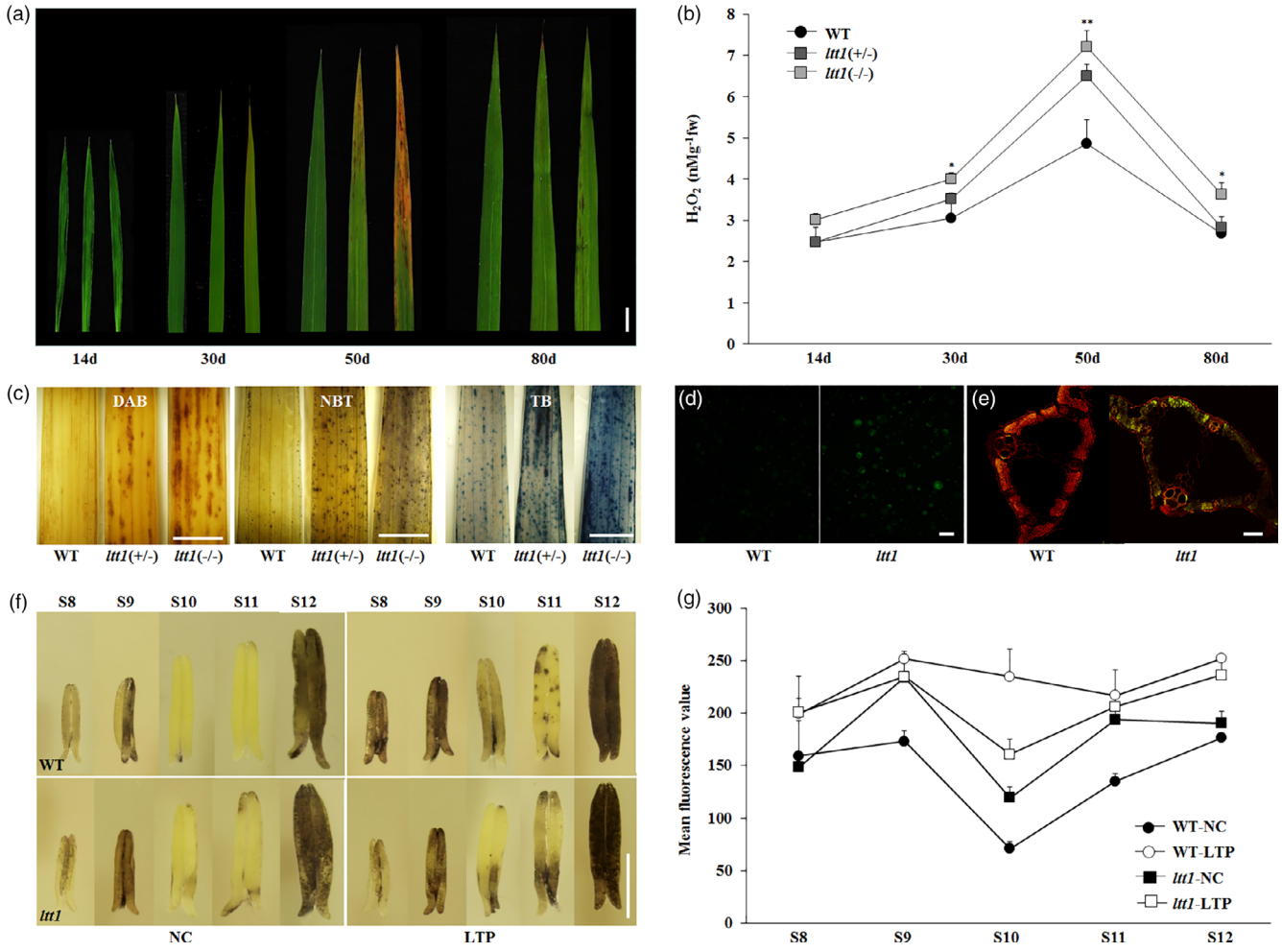

FIGURE 2 *ltt1* shows increased endogenous ROS content. (a) The lesion mimic phenotype in the fully opened leaves of WT (left), *ltt1*(+/−; middle), and *ltt1*(−/−; right) at the indicated stages, respectively. Bar = 1 cm. (b) H_2O_2 quantification on the leaves shown in (a). Data are means ± *SD* (*n* = 3). **p* < .05, ***p* < .01 (Student's *t*-test). (c) 3,3'-Diaminobenzidine, nitroblue tetrazolium, and trypan blue staining for the visualization of H_2O_2, O^{2-}, and membrane damage, respectively. Newly opened leaves were sampled from 50-day-old plants grown under natural conditions. Bar = 1 cm. (d) H_2DCF-DA staining for the visualization of intracellular ROS content. Seedlings of 14 days after sowing (DAS) were sampled for protoplast extraction. Green florescence indicates ROS-positive signals. Bar = 50 μm. (e) Terminal deoxynucleotidyl transferase-mediated dUTP nick end labelling assay. Red fluorescence indicates the cell nucleus stained by propidium iodide, and yellow fluorescence indicates the terminal deoxynucleotidyl transferase-mediated dUTP nick end labelling-positive signals. Bar = 100 μm. (f) Nitroblue tetrazolium staining for the visualization of O^{2-}. The anthers of *ltt1* and WT under normal and cold stress conditions were sampled at different developmental stages. Bar = 1 mm. (g) Reactive oxygen species level evaluated by mean fluorescence value using H_2DCF-DA staining. The anthers at the indicated stages were sampled for analysis. Data are means ± *SD* (*n* = 3). LTP, low temperature under phytotron conditions; NC, normal conditions; WT, wild type [Color figure can be viewed at wileyonlinelibrary.com]

signalling molecule to induce timely tapetal PCD (Ko et al., 2017; Luo et al., 2013; Yi et al., 2016). Under cold stress, the intracellular ROS level would dramatically increase, and maintaining ROS homeostasis therefore appears to associate intimately with the adaptation to extreme temperature in rice (Baxter et al., 2014; Zhang et al., 2016). Because *ltt1* shows increased endogenous ROS level, we speculate that the elevated ROS content in vivo may help the mutant buffer the ROS burst induced by low temperature. To confirm this hypothesis, we performed NBT and H_2DCF-DA staining to detect ROS dynamics at various stages of anther development under cold stress and normal conditions, respectively. Compared with those developed under normal conditions, we observed intense NBT signals in the cold-stressed anthers of WT at Stage 8, and the signal intensity remained high at Stages 9 and 10 (Figure 2f). By contrast, the increase in signal intensity was much lower in cold-stressed anthers of the mutant at the same developmental stages (Figure 2f). We further performed H_2DCF-DA fluorescence intensity quantification in the cold-treated and untreated anthers. Although the ROS content was also somewhat increased in the mutant after cold treatment, the increase was much lower compared with the significant change of ROS level between the cold-treated and untreated anthers in the WT (Figure 2g). These observations suggest that *ltt1* could maintain well the ROS homeostasis during anther development after suffering from cold stress.

Previous studies have shown that excessive accumulation of ROS might lead to premature tapetal PCD and thus pollen sterility (Ko et al., 2017; Luo et al., 2013). To understand whether the cold-induced ROS burst in the WT triggers abnormal tapetum degradation, we examined the dynamic development of tapetum and microsporocyte by series transverse sections. Under normal conditions, no obvious difference could be observed between *ltt1* and WT in microspore development and tapetum degradation (Figure S6a). For both materials, tapetal cells started to initiate degradation at Stage 8 and became vacuolated and shrunken with darkly stained cytoplasm. At Stage 9, tapetal cells underwent drastic degradation and became much vacuolated and displayed a ridge-like shape. When developed to Stage 10, tapetum became less vacuolated and condensed like a loop but was still strongly stained. The tapetum almost disappeared at Stage 11, and the round-shaped pollen grains full of reserve substances were clearly visible at Stage 12. For the *ltt1* mutant, there was no detectable difference in the development of anthers under normal and cold stress conditions (Figures 3a and S6a). In the WT, the anthers showed nearly normal tapetum morphology and microspore development at Stage 8 under cold stress (Figure 3a). However, when reaching to Stage 9, cold-stressed tapetal cells of WT exhibited dramatic degradation, and the tapetum became accelerately condensed, fine striped, or even broke. At the early Stage 10, tapetal cells were barely visible, and the epidermal layer of tapetum became distorted. From the late Stage 10 to Stage 12, locules of the cold-stressed anthers in the WT were shrivelled, and some even became ruptured with deformed and aborted microspores. Totally, these results indicate that the low-temperature-induced ROS burst accelerates the degradation of WT tapetum, resulting in the decrease of pollen fertility and seed setting rate.

To further confirm the relationship between ROS burst and accelerated tapetum degradation in the WT anthers under cold stress, we conducted TUNEL assay for the anthers collected from Stages 7 to 12 under both normal and cold stress conditions. We found that yellow-coloured TUNEL signals could be first detected in the tapetum at Stage 8, and the signal intensity in tapetal cells increased at Stage 9 (Figure S6b). Dense and intensive TUNEL signals could be observed in the degenerating tapetal cells at Stage 10 and were nearly undetectable at Stage 11–12. No any obvious difference of PCD signals was observed between *ltt1* and WT during the whole pollen developmental stages under normal growth conditions (Figure S6b). The cold-stressed anthers of *ltt1* showed PCD signals completely the same as that in the normal-growing anthers at each pollen developmental stage (Figures 3b and S6b). By contrast, TUNEL signals were also first observed at Stage 8 in the cold-treated anthers of WT, but the signal intensity was abruptly enhanced in the tapetal cells at Stage 9 compared with that under normal conditions (Figures 3b and S6b), indicating accelerated tapetal PCD. In addition, intense TUNEL signals could still be observed in degenerating tapetal fragments and aborted microspores after Stage 9 and were even present in the locules disrupted in structure at Stage 12. Taken together, these results suggest that in contrast to the accelerated tapetum degradation caused by cold-induced ROS burst in the WT, the slight change of ROS content in the cold-stressed anthers of *ltt1* enabled the mutant to maintain relatively normal tapetal PCD, thus ensuring the formation of pollen grains with normal function.

3.4 | *ltt1* shows differential expression of ROS homeostasis genes and tapetal PCD genes

The ROS amount in plant cells under stress conditions is dynamically controlled by the regulatory networks of ROS-generating system and ROS-scavenging system (Choudhury et al., 2017; Dreyer & Dietz, 2018). Plant respiratory burst oxidase homologs, also known as NADPH oxidases, are the most crucial enzymes in ROS-producing system (Ben Rejeb et al., 2015; Marino, Dunand, Puppo, & Pauly, 2012; Suzuki et al., 2011). The rice genome contains nine *Rbohs* (Kaur et al., 2018), we found that except the three genes of *OsRboh6*, *OsRboh8*, and *OsRboh9*, the other six *OsRbohs* showed significantly enhanced expression in the anthers of *ltt1* (Figure 4a), which should be largely responsible for the over accumulated ROS in the mutant.

If kept unchecked, the highly enhanced expression of genes involved in ROS production in *ltt1* would result in ever increasing ROS concentrations in the cells, which would lead to the oxidative destruction of the cell and finally seedling death (Choudhury et al., 2017), because *ltt1* could survive well under a high level of endogenous ROS, suggesting that the ROS over-producing process must be mitigated by the detoxifying proteins such as SOD, ascorbate peroxidase, catalase isozyme, and glutathione peroxidase (Choudhury et al., 2017; Dreyer & Dietz, 2018; Mittler, 2017). To confirm this hypothesis, we investigated the expression of the related protein coding genes in *ltt1* and WT. Because the rice genome contains eight putative *APXs*, seven putative *SODs*, three putative *CATs*, and five putative *GPXs*, we selected three genes from each family based on existing reports or rice expression profile database (http://ricexpro.dna.affrc.go.jp/) and compared their expression levels between *ltt1* and WT. We found that transcription of most of the genes involved in ROS scavenging was significantly increased under the mutant background (Figure 4b). And expression profile of the three catalase genes in *ltt1* was highly consistent with that in rice leaves under water stress (Ye, Zhu, Liu, Li, & Zhang, 2011), which should contribute to the prevention of excessive ROS accumulation. We also detected the expression of the three alternative oxidase genes (AOX) contained in the rice genome because they are cold responsive and function in the chilling tolerance of rice seedlings (Ito, Saisho, Nakazono, Tsutsumi, & Hirai, 1997; Li et al., 2013). We found that the expression level of *AOX1a* and *AOX1b* in *ltt1* was more than 20 times higher than that in WT (Figure 4c). Because the activities of SODs and peroxidases appear to correlate positively with cold tolerance in rice (Kim, Choi, Cho, & Kim, 2011; Lee, Kwon, & Kim, 2009; Liu et al., 2018), we further detected the activity of the related enzymes in *ltt1* and WT. The results showed that the activities of these enzymes in the mutant plants increased significantly (Figure 4d,e), which may help the mutant to eliminate the excessive ROS more effectively.

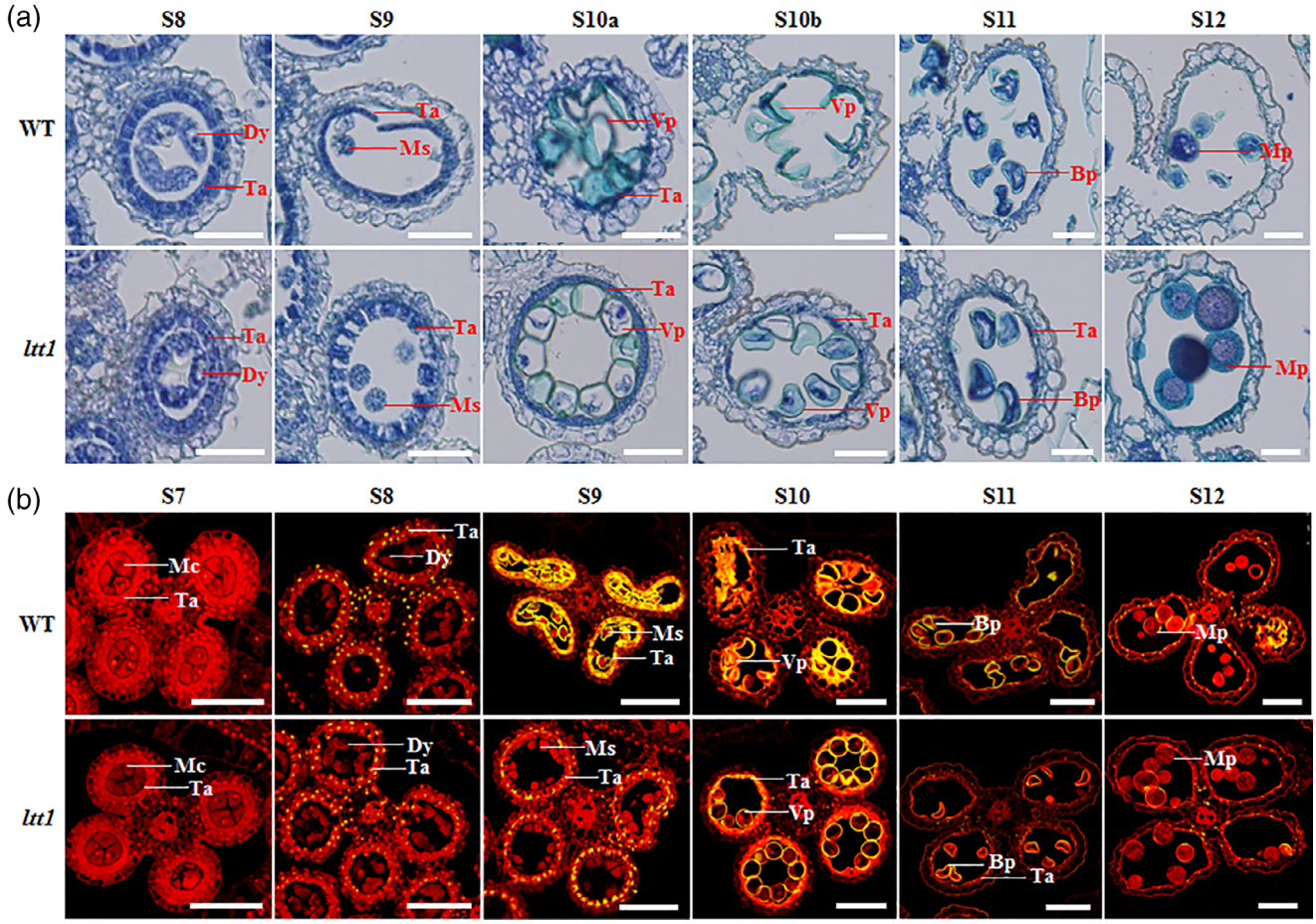

FIGURE 3 *ltt1* shows normal tapetal programmed cell death under cold stress conditions. (a) Tapetal programmed cell death observation. The anthers of *ltt1* and WT under cold stress conditions were sampled at different developmental stages. Bars = 50 μm. (b) Terminal deoxynucleotidyl transferase-mediated dUTP nick end labelling assay. The anthers of *ltt1* and WT under cold stress conditions were sampled at different developmental stages. Red fluorescence indicates the cell nucleus stained by propidium iodide, and yellow fluorescence indicates the terminal deoxynucleotidyl transferase-mediated dUTP nick end labelling-positive signals. Bars = 100 μm. Bp, bicellular pollen; Dy, Dyad cell; Mc, meiotic cell; Mp, mature pollen; Ms, microspore; Ta, tapetum; Vp, vacuolated pollen; WT, wild type [Color figure can be viewed at wileyonlinelibrary.com]

The enhanced transcription of genes involved in ROS scavenging and the elevated activity of related enzymes suggest that the antioxidant system is highly activated in the mutant. We therefore performed H_2O_2 treatment to confirm this speculation. After treating the 30-day-old seedlings with 80-mM H_2O_2 for 10 days, we found that the leaves of WT displayed severe necrosis and then gradually withered (Figure 4f). After 7 days of recovery, the survival rate of WT was only about 42%, in contrast to approximately 75% of that of *ltt1* (Figure 4g), demonstrating that the *ltt1* plants had strong adaptability to oxidative stress.

ROS are important signalling molecules necessary for multiple biological processes (Mittler, 2017) and play a key role in tapetal PCD (Yu et al., 2017). Failure to remove the excessively accumulated ROS in the tapetum would result in male sterility by causing precocious tapetal PCD (Hu et al., 2011; Luo et al., 2013; Xie et al., 2014). To understand the molecular mechanism of excessive ROS production in affecting tapetum degradation under cold stress conditions, we first detected the expression of *OsRbohs* in cold-stressed anthers at Stage 9. Consistent with the differential changes of the endogenous ROS level induced by cold stress between the mutant and WT, we found that transcription of *OsRbohs* was all greatly induced in the cold-stressed anthers of WT, whereas expression of most of these genes was only slightly changed in the anthers of *ltt1* under the same cold stress conditions (Figures 4a and S7a). We then surveyed the expression of 11 tapetal PCD genes in the anthers of *ltt1* and WT, including *OsUDT1* (Jung et al., 2005), *OsTDR1* (Li et al., 2006), *OsMYB80/OsMYB103* (Phan, Li, & Parish, 2012), *OsMADS3* (Hu et al., 2011), *OsPTC1* (Li et al., 2011), *OsEAT1/DTD* (Ji et al., 2013; Niu et al., 2013), *OsTIP2* (Fu et al., 2014; Ko et al., 2014), *OsDTC1* (Yi et al., 2016), *OsTGA10* (Chen et al., 2018; Yang et al., 2016), and *OsAGO2/OsHXK1* (Zheng et al., 2019). We found that under natural growth conditions, some of the tapetal PCD genes, including *OsAGO2* and its downstream target *OsHKX1*, *OsMYB80*, and *OsUDT1*, showed enhanced expression in *ltt1* compared with that in WT (Figure 4h), which should be due to the inductive effects of the elevated ROS level in the mutant. When encountering low temperature at Stage 9, 9 out of the 11 genes showed significantly upregulated expression in the anthers of WT. By contrast, expression of most of these genes

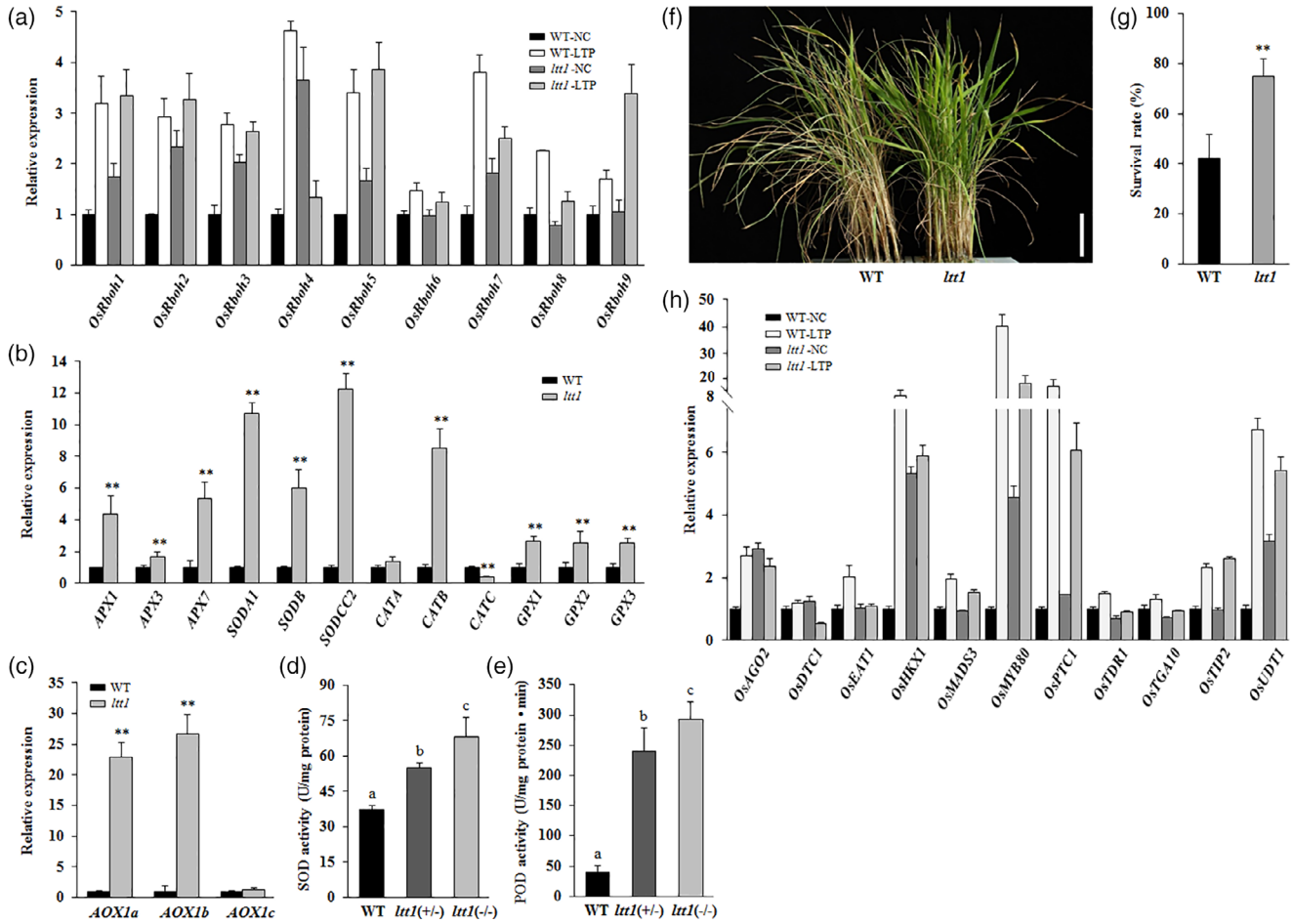

FIGURE 4 *ltt1* shows differential expression of reactive oxygen species (ROS) homeostasis genes and tapetal programmed cell death genes. (a–c) Expression analysis of genes involved in ROS production and ROS scavenging. (a) Anthers at Stage 9 were collected from plants grown under NC and LTP. (b,c) Newly opened leaves were sampled from 50-day-old plants grown under natural conditions. The transcript levels were normalized against WT-NC (a) and WT (b,c), which were set to 1. Data are means ± *SD* ($n = 3$). $^{**}p < .01$ (Student's *t*-test). (d,e) Enzyme activity quantification. Newly opened leaves of 60-day-old plants under natural conditions were sampled for analysis. Data are means ± *SD* ($n = 3$). Bars followed by different letters indicate significant difference at 5%. (f,g) *ltt1* displays oxidative stress tolerance. Seedlings that are 30 days old were treated with 80-mM H_2O_2 for 10 days. Data are means ± *SD* ($n = 3$). Bar = 5 cm. $^{**}p < .01$ (Student's *t*-test). (h) Expression analysis of tapetal programmed cell death genes. Anthers at Stage 9 were collected from plants grown under NC and LTP. The transcript levels were normalized against WT-NC, which was set to 1. Data are means ± *SD* ($n = 3$). LTP, low temperature under phytotron conditions; NC, normal conditions; WT, wild type [Color figure can be viewed at wileyonlinelibrary.com]

did not change significantly in cold-stressed mutant anthers, or the variation of gene expression was much moderate than that in WT (Figures 4h and S7b). These results suggest that *LTT1* has critical functions in ROS-mediated regulatory network for tapetal PCD under cold stress conditions.

3.5 | Identification of the causal mutation

To understand further the function of *LTT1* in cold tolerance, we performed map-based cloning to isolate the underlying gene. Using 50 bulked WT and *ltt1*(−/−) plants sampled from the F_2 population of *ltt1* and KY131 (*japonica*), respectively, the candidate was roughly mapped to the region between markers M1 and M6 on the long arm of chromosome 10 (Figure 5a). Further analysis using 1,041 mutant plants located the candidate to a 55-kb region between makers M8 and M10. This region contains nine putative ORFs (http://rice.plantbiology.msu.edu/), and sequencing of the whole 55-kb fragment detected a mutation of C to T in the coding region of *Os10g34110*, which caused an amino acid change from His to Tyr.

To confirm that the C/T substitution is responsible for the mutant phenotype, we first genotyped the 376 plants derived from the self-fertilized *ltt1*(+/−) plants using the mutation-specific dCAPS marker (Table S1). We found that the three genotypes of CC, CT, and TT were completely linked with the phenotypes of WT, *ltt1* (+/−), and *ltt1*(−/−), respectively. Because *ltt1* shows semi-dominant feature in all agronomic traits including cold-stressed seed setting

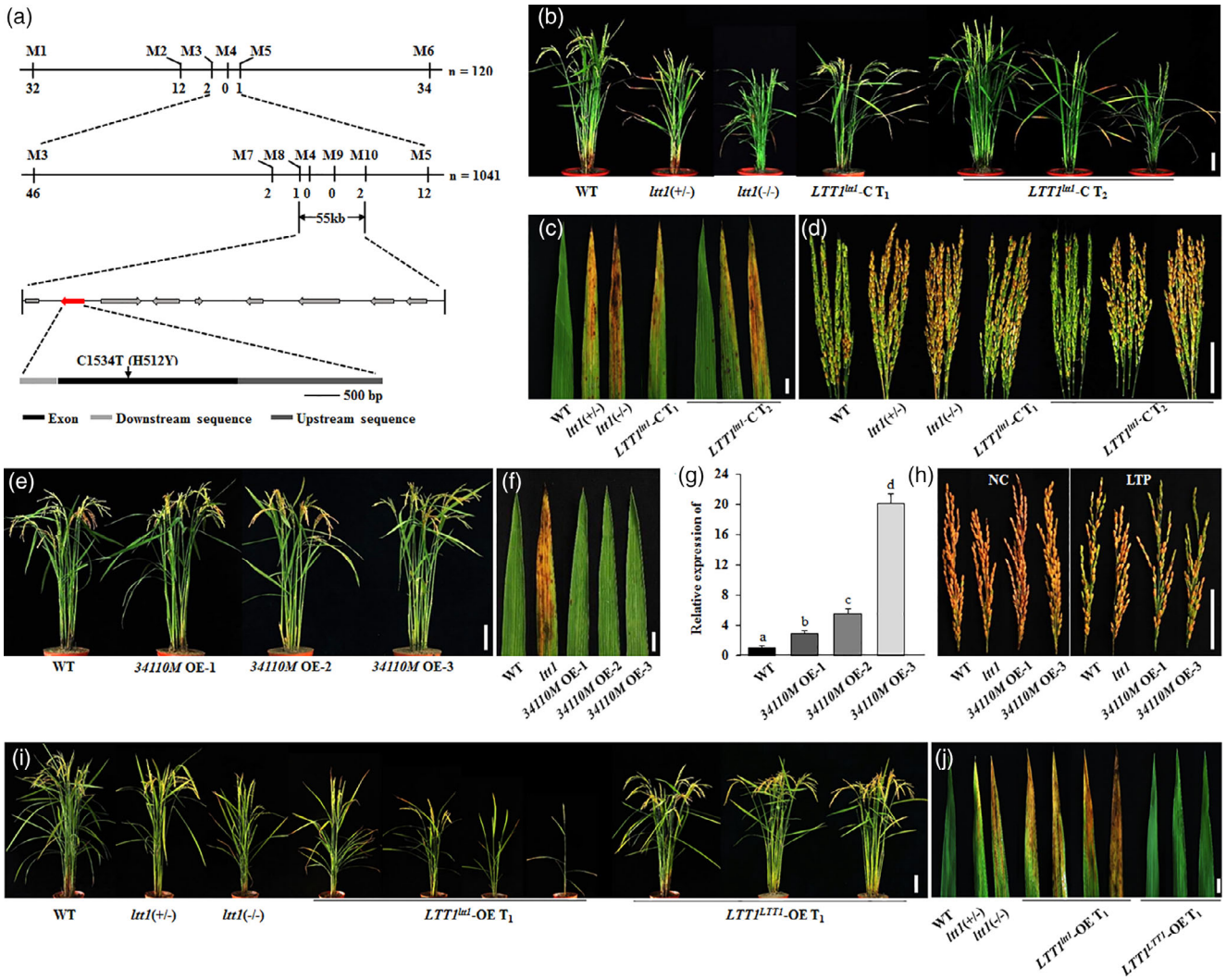

FIGURE 5 Identification of the causal mutation. (a) Fine mapping of the causal mutation. Indicating a C/T point mutation occurred in the annotated *Os10g34110* gene. (b–d) Complementation test. Showing the complemented mutant phenotype of plant height (b), lesion mimic leaves (c), and cold-stressed seed setting under the WT background (d). Bars = 10 (b), 1 (c), and 5 cm (d). (e–h) Functional test of *Os10g34110*. The *34110M* OE indicates that the mutation-containing coding sequence of *Os10g34110* was overexpressed under the WT background. Showing that the differentially overexpressed *34110M* transgenic lines (g) displayed the WT morphology in overall traits including the whole plant (e), leaves (f), and cold-stressed seed setting (h). Bars = 10 (e), 1 (f), and 5 cm (h). (g) The transcript levels were normalized against WT, which was set to 1. Data are means ± *SE* (*n* = 3). Bars followed by different letters indicate significant difference at 5%. (i–j) Overexpression assay. $LTT1^{ltt1}$-OE and $LTT1^{LTT1}$-OE indicate that the 5,561-bp genomic DNA amplified from *ltt1* and WT, respectively, was overexpressed under the WT background, showing that the $LTT1^{ltt1}$-OE transgenic lines displayed *ltt1*-like phenotypes including plant height, tiller number, and lesion mimic leaves, whereas the $LTT1^{LTT1}$-OE transgenic plants all showed overall traits similar to that of the WT. Bars = 10 (i) and 5 cm (j). WT, wild type [Color figure can be viewed at wileyonlinelibrary.com]

(Figure S2), we performed a genetic complementation test by introducing the 5,561-bp genomic DNA fragment of *Os10g34110* amplified from *ltt1* into the background of WT. All the 35 independent T_1 transgenic lines showed overall phenotypes, including the lesion mimic leaves and the higher seed setting under cold stress, which resembled that of the *ltt1*(+/−) plant (Figures 5b–d and S8). And the self-fertilized T_2 generation segregated into three types, with overall morphology similar to that of WT, *ltt1*(+/−), and *ltt1*(−/−), respectively (Figures 5b–d and S8). This result clearly demonstrates that the mutation-containing 5,561-bp genomic DNA is responsible for the *ltt1* phenotype.

3.6 | The *ltt1* phenotype is not caused by dysfunction of the annotated *Os10g34110* gene

The mutation in *LTT1* displays stronger effects on booting stage cold tolerance than all the other genes identified so far (Liu et al., 2019; Saito et al., 2010; Zhang et al., 2017). However, the increase of ROS content in vivo caused by the mutation also shows negative effects on the development of some other traits including lesion mimic leaves and reduced tiller number (Figures S2d and S5b). Because *LTT1* shows dosage-dependent effects on cold tolerance and other agronomic traits (Figures S2 and S5), we assume that it is possible to obtain

transgenic plants with enhanced cold tolerance and relative normal development of other traits by properly downregulating the expression of the causal gene. Therefore, we tried to reduce the transcripts of *Os10g34110* using the RNA interference (RNAi) approach. Among the 45 independent transgenic T_3 lines, we selected three homozygotes with differentially downregulated expression of *Os10g34110* for further analysis (Figure S9c). Very surprisingly, the appearance of all three kinds of transgenic plants, including leaf morphology, was exactly the same as that of the WT plants, regardless if the reduction of the transcripts was more or less (Figure S9a–c). And the sensitivity of *34110* RNAi lines to cold stress at the booting stage was also similar to that of WT (Figures S9d and S8).

Because it is are unclear whether the normally developed phenotypes of these *34110*-RNAi plants is due to the insufficient downregulation of the expected causal gene, we tried to knockout the *Os10g34110* locus under the WT background using the CRISPR/Cas9 plant genome editing system. By editing specifically the target site near the start codon, we obtained a series of transgenic plants with diverse insertion or deletion in the coding region and selected two representative lines of *34110* KO-1 and *34110* KO-2 (Figure S10a), which encode a frame-shifted/truncated 34110 protein of 261 and 90 residuals, respectively, for phenotypic analysis. Unexpectedly, no any *ltt1*-like agronomic traits, including the lesion mimic leaves and cold-stressed seed setting, were observed in the two transgenic plants (Figures S9e–g and S8). Crossing the *34110* KO plants with *ltt1*(−/−) revealed that the resultant F_1 plants showed overall phenotypes similar to that of the *ltt1*(+/−) plants (Figures S9e–g and S8), indicating that the existence of the point mutation could still lead to the mutant phenotype even in the absence of *Os10g34110* function.

Numerous studies have shown that small RNAs and non-coding RNAs are involved in various stress response processes (Li, Castillo-Gonzalez, Yu, & Zhang, 2017; Wang, Meng, Dobrovolskaya, Orlov, & Chen, 2017a). To study whether the C/T mutation occurs on unknown small molecules or key cis-acting regulatory elements, we designed primers to edit the target site nearby the point mutation (Figure S10b). Disappointedly, introducing of the edited sequences into WT could not yet yield any plants that could mimic the mutant phenotype (Figures S9e–g and S8).

Because the 5,561-bp genomic fragment from *ltt1* could endow WT with phenotypes similar to that of the mutant (Figure 5b–d), we further carried out overexpression experiment under the background of WT using the ubiquitin promoter-driven mutated transcripts (*34110M* OE), thus expected to obtain a gain of function mutant phenotype. Although we enhanced the transcription of *34110M* to about 20 times more than that of WT, the transgenic plant still displayed complete WT phenotypes (Figure 5e–h). This result makes us suspect that this 5,561-bp genomic fragment might contain a functional transcript that is not predicted in the current database. Therefore, we performed a comparative experiment by overexpressing this 5,561-bp fragment amplified from *ltt1* ($LTT1^{ltt1}$-OE) and WT ($LTT1^{LTT1}$-OE) under the background of WT. Similar to that observed in the complementation test, 20 out of the 25 independent $LTT1^{ltt1}$-OE T_1 transgenic lines showed *ltt1*-like lesion mimic leaf phenotype (Figure 5i,j). Furthermore, consistent with the dosage effects of the 5,561-bp fragment on overall traits (Figure 5b–d), we observed considerable phenotypic variations including plant height, tiller number, and lesion area among the $LTT1^{ltt1}$-OE T_1 transgenic lines (Figure 5i,j). By contrast, all the 45 $LTT1^{LTT1}$-OE T_1 transgenic plants showed phenotypes completely the same as that of the WT (Figure 5i.j). Taken together, these results suggest that the 5,561-bp fragment contains a novel transcript responsible for the *ltt1* mutant phenotype.

3.7 | *ltt1* shows great potential in cold tolerance breeding

DHX is the major cultivar in the first accumulative temperature zone of Heilongjiang province, the northernmost part of China vulnerable to low-temperature stress. Because of the good eating quality, DHX is highly welcomed by the consumers, with the price of about five times than that of the others in the rice market. However, despite that DHX harbours the cold-tolerant allele of *CTB4a* (Hap1; Zhang et al., 2017), this variety is highly sensitive to cold stress at the booting stage, and extension of DHX is therefore strictly limited to the region with the accumulative temperature of more than 2,800°C. Therefore, we tried to introduce the *ltt1* mutation into the DHX background to explore the potential value of *ltt1* in practical production. Because the mutation in *LTT1* delays heading date by about 15 days, we first crossed DHX with LJ31, a cultivar carrying the Mudanjiang8 allele of *Ghd7* (Xue et al., 2008) and the A4 allele of *DTH2* (Wu et al., 2013), to substitute for the Nipponbare allele and the A2 allele in the DHX background, respectively (Figure S11a,b). The near isogenic line containing the two alleles of *DTH2* and *ghd7* (NIL-*DTH2-ghd7*; NIL-*Dg*) displayed a heading date of about 20 days earlier than that of DHX (Figure 6a,b). We then introduced the *ltt1* allele into the *NIL-Dg* background (Figure S11c), and the obtained pyramided line (NIL-*DTH2-ghd7-ltt1*; NIL-*Dgl*) showed a heading date nearly the same as that of DHX (Figure 6a,c). Investigation of the cold-stressed seed setting found that DHX, as well as the NIL-*Dg* plants, were all highly sensitive to low-temperature stress, with the seed setting rate of no more than 20% under cold stress conditions (Figure 6a–d). In contrast, the NIL-*Dgl* plants displayed a setting rate of about 60%, and grain yield of these plants was thus greatly increased under the same stress conditions (Figure 6d,e). This observation further demonstrates the pivotal role of the *ltt1* mutation in cold tolerance.

The mutation in *LTT1* shows adverse effects on tiller number per plant (Figure S5), one of the key factors determining grain yield. However, the unfavourably affected trait by *ltt1* is purely from the view of functional genomics, that is, emphasis on the tillering ability of each individual plant. In actual production, however, regardless if transplanted manually or mechanically, there are at least 3–5 seedlings in each point. Therefore, the impact of *ltt1* on grain yield under normal conditions needs to be evaluated by conventional farming methods. Moreover, the difference in tillering ability among cultivars could also be reduced by changing the planting density (Sakamoto et al., 2006). From the perspective of application, we designed three

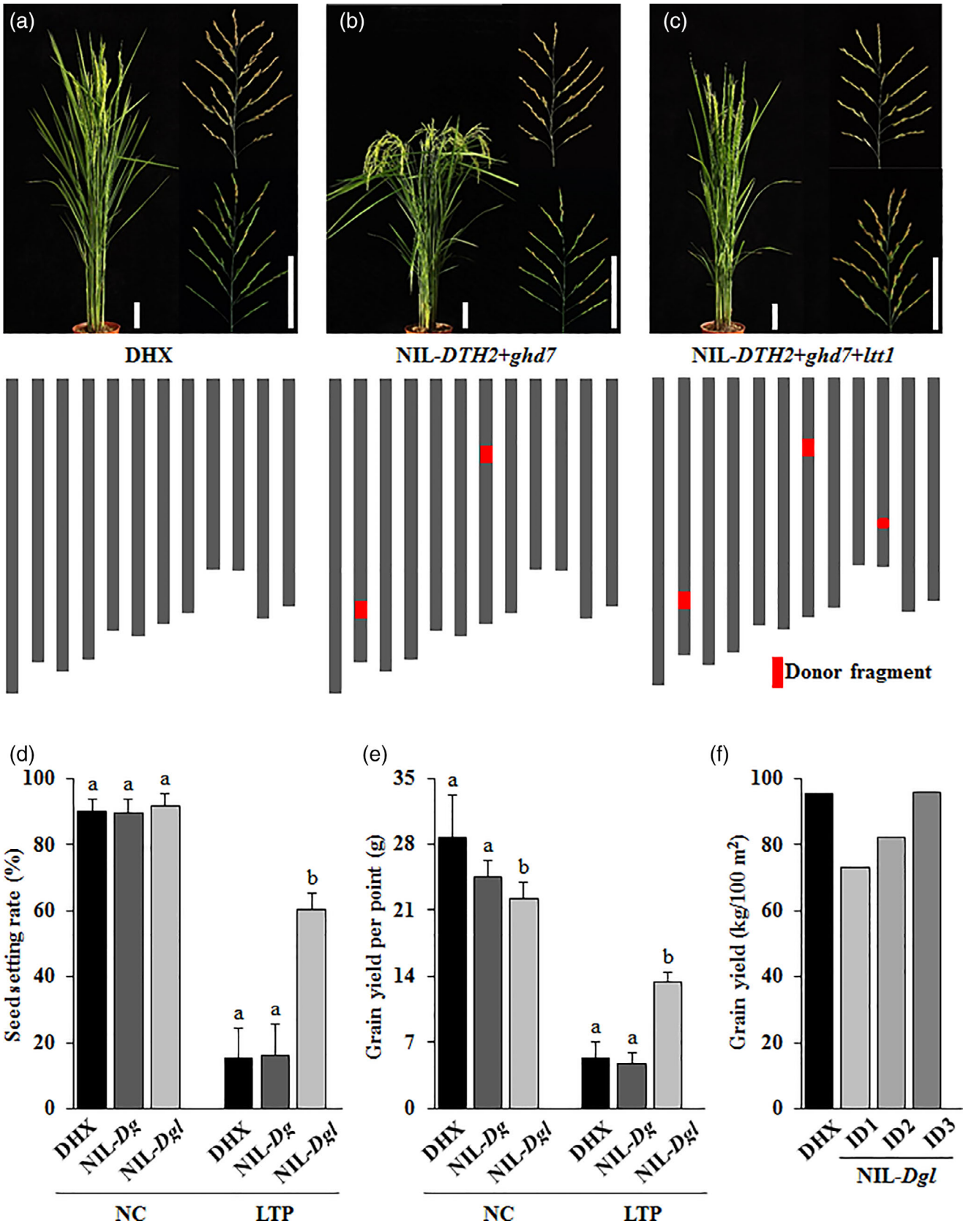

FIGURE 6 Legend on next page.

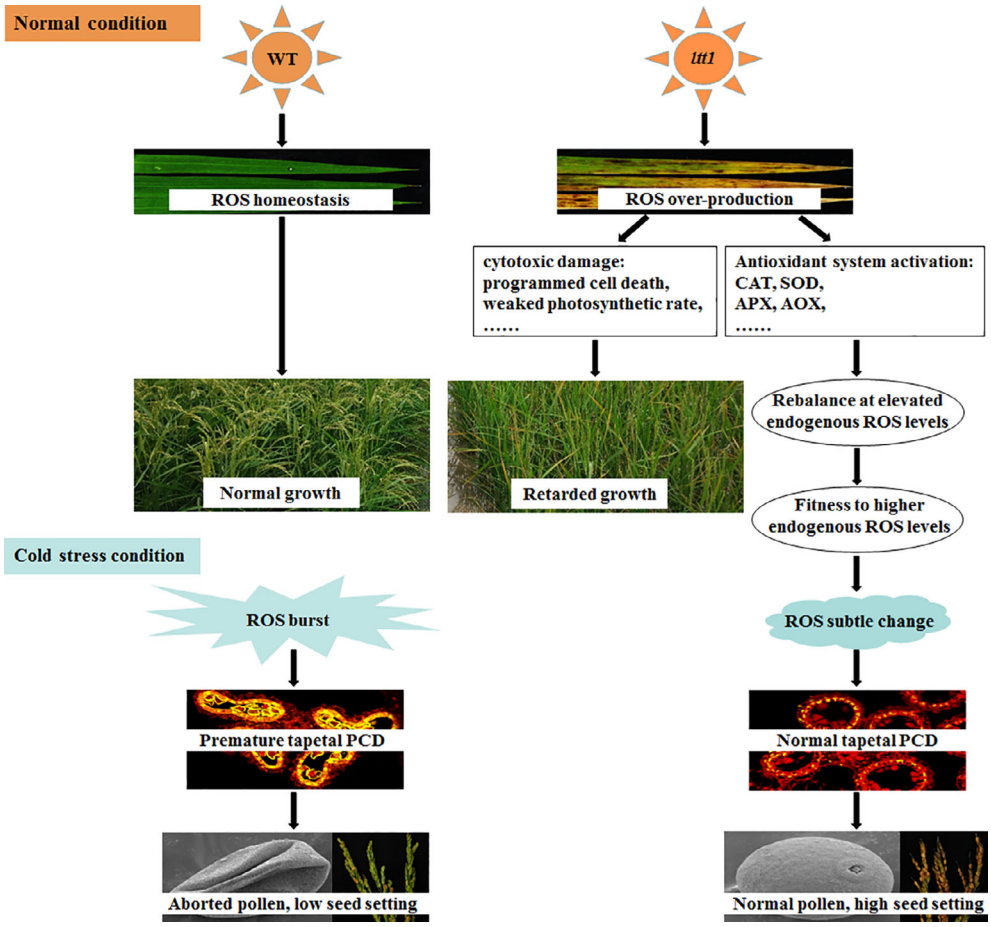

FIGURE 7 Proposed model for the function of *LTT1* in booting stage cold tolerance in rice. AOX, oxidase genes; APX, ascorbate peroxidase; CAT, catalase isozyme; SOD, superoxide dismutase; PCD, programmed cell death; ROS, reactive oxygen species [Color figure can be viewed at wileyonlinelibrary.com]

cultivation models of 20 × 20 cm (the ideal planting density for DHX), 17 × 16 cm, and 15 × 12 cm to observe the productivity of NIL-*Dgl*. We found that the grain yield of NIL-*Dgl* was about 76% that of DHX under the 20 × 20 cm cultivation method (Figure 6f). When increasing the planting density from 20 × 20 cm to 15 × 12 cm, the yield performance of NIL-*Dgl* reached to about the same level as that of DHX (Figure 6f), suggesting that *ltt1* has great potential in cold tolerance breeding under suitable cultivation manner.

4 | DISCUSSION

Low temperature is a major factor limiting rice productivity and geographical distribution. However, compared with other agronomic traits, the evaluation of cold tolerance at the booting stage is particularly difficult. Consequently, few reliable genes/QTLs have so far been identified, and the molecular mechanism of plant cold tolerance at the boot stage is still poorly understood. In this study, we show that the *LTT1*-mediated ROS homeostasis is critical for cold tolerance of rice plants at the booting stage. Although *ltt1* shows adverse effects on other agronomic traits including heading date and tiller number per plant, pyramiding of other elite genes with *ltt1* improves greatly the cold stress tolerance of the recipient variety without yield penalty under suitable cultivation measure (Figure 6). In addition, except for the reduced tiller number per plant, the *ltt1*(+/–) plants shows strong cold tolerance and displays no other unfavourable traits under normal conditions (Figures S2 and S5), suggesting the potential value of *ltt1* in heterosis utilization. Therefore, our study identifies a valuable gene

FIGURE 6 *LTT1* shows great potential in cold tolerance breeding. (a–c) Plant morphologies and chromosome maps of DHX, NIL-*DTH2* + *ghd7* (NIL-*Dg*), and NIL-*DTH2* + *ghd7* + *ltt1* (NIL-*Dgl*). Bars = 10 cm. The shorter vertical bar is for plant, and the longer vertical bar is for panicle. The inner panels indicate the panicles collected from plants grown under NC (upper) and LTP (lower), respectively. Indicating no obvious difference in the heading date between DHX and NIL-*Dgl*. (d) Comparison of seed setting in DHX, NIL-*Dg*, and NIL-*Dgl* under normal and cold stress conditions, respectively. Data are means ± *SD* (*n* = 10). Bars followed by different letters indicate significant difference at 5%. (e) Comparison of grain yield per point between DHX and NIL-*Dgl* under normal and cold stress conditions, respectively. Three plants were transplanted for each point. Data are means ± *SD* (*n* = 5). Bars followed by different letters indicate significant difference at 5%. (f) Comparison of grain productivity between DHX and NIL-*Dgl* under different planting density. Three plants were transplanted for each point. The planting density for DHX is the same as ID1 (20 × 20 cm), and ID2 and ID3 indicate the densities of 17 × 16 cm and 15 × 12 cm, respectively. LTP, low temperature under phytotron conditions; NC, normal conditions [Color figure can be viewed at wileyonlinelibrary.com]

resource that could be applied in practical cold tolerance breeding in rice.

The normal development of pollen grains depends on the timely initiation and normal execution of tapetum degeneration, both of which are affected by the temporal and spatial dynamics of ROS (Luo et al., 2013; Yi et al., 2016; Zheng et al., 2019). However, little is known about how cold stress influences tapetal PCD and pollen fertility by altering the ROS homeostasis in anthers. In this paper, we found that the ROS level was dramatically increased in the anthers of WT but remained relatively stable in those of *ltt1* when plants were exposed to cold stress at the booting stage (Figure 2f,g). Hence, an important question is why does ROS content only change slightly in the cold-stressed mutant plants? Previous research revealed that cold-primed plants could accumulate numerous elicitors including ROS, which help plants acquire a long-term or transient stress memory to improve the tolerance to the coming chilling stress and may provide ultimately a mechanism for cold acclimation and adaptation (Avramova, 2015; Baier, Bittner, Prescher, & van Buer, 2019; Friedrich, Faivre, Bäurle, & Schubert, 2018). Similarly, hydrogen peroxide priming could also improve chilling tolerance of the plant by activating ROS detoxification and scavenging systems (Hossain et al., 2015). And the ROS metabolism system appears to be the target of selection during the divergence of the two rice subspecies of chilling-tolerant *japonica* and chilling-sensitive *indica*, with the former containing much higher endogenous ROS level and earlier accumulation of antioxidative components when encountering cold stress (Zhang et al., 2016). In this study, we found that the endogenous ROS level of *ltt1* was significantly higher than that of WT under normal growth conditions (Figure 2), indicating that the mutant was under consistent oxidative stress. Consequently, the adaptation to high endogenous ROS level allowed the mutant to resist oxidative stress, as revealed by the H_2O_2 treatment (Figure 4f,g). Obviously, to prevent oxidative damage of the cells (Choudhury et al., 2017), the mutant effectively activated the ROS production system as well as the antioxidant system (Figure 4), resulting in the establishment of cellular ROS homeostasis at a higher level (Figure 2), which helps the plants to buffer the rise of ROS level when encountering cold stress (Figure 2f,g). Therefore, our results demonstrate that the *LTT1*-mediated pathway is critical for the activation of in vivo ROS metabolism system.

The highly enhanced booting stage cold tolerance of the mutant suggests that the activation of ROS metabolism system is beneficial for plants to cope with the coming cold stress. We propose a model to summarize our hypothesis for the function of *LTT1* in rice (Figure 7). *LTT1* plays a pivotal role in ROS homeostasis by regulating the expression of multiple genes involved in ROS production and ROS scavenging. The point mutation in *LTT1* leads to a dramatic increase in endogenous ROS level (Figure 2), which produces toxic effects on various developmental processes (Figure S2). To avoid oxidative destruction to the cells, the mutant establishes a novel ROS homeostasis at a higher level by activating various antioxidant systems (Figure 4), and the *ltt1* plants acclimated under elevated ROS level acquire a long-term oxidative stress memory by remodelling ROS-mediated regulatory networks. Under low temperature stress conditions, the cold-induced ROS burst would occur in the anthers of WT (Figure 2f,g), thus triggering the expression of tapetal PCD genes (Figure 4h), accelerating tapetal PCD and ultimately leading to pollen abortion (Figure 3). In contrast, the acclimation to oxidative stress enables the mutant to maintain a relatively stable level of endogenous ROS (Figure 2f,g). Therefore, the subtle change in ROS level during cold stress would not severely affect the expression of tapetal PCD genes (Figure 4h), and the tapetal PCD in the mutant could thus proceed normally (Figure 3), which gives the mutant higher pollen fertility and seed setting rate. Therefore, although the increase of ROS content has downside for the timely degradation of tapetum (Hu et al., 2011; Luo et al., 2013; Xie et al., 2014; Zheng et al., 2019), our results uncover that the acclimation of rice plants to elevated endogenous ROS level is critical for cold tolerance at the booting stage.

Our complementation test, overexpression assay, and the cold-tolerant phenotype of NIL-*Dgl* plants selected with the mutation-based specific marker clearly demonstrated the function of the mutation-containing 5,561-bp genomic DNA in booting stage cold tolerance (Figures 5b–d,i–j and 6d). Unexpectedly, although multiple genetic approaches have been adopted, we failed to determine the molecule responsible for the cold tolerant *ltt1* phenotype. Apparently, *Os10g34110* is not the gene causing the mutant phenotype (Figures 5e–h and S9), and the edited insertion/deletion nearby the C/T mutation also excludes the possibility of the existence of small molecules or key cis-acting regulatory elements (Figure S9e–g). Further studies should be carried out to identify the underlying transcript responsible for the *ltt1* mutant phenotype.

In conclusion, the point mutation in *LTT1* plays a crucial role in the activation of in vivo ROS metabolism system, which is of great significance to prevent the excessive production of ROS induced by low temperature and maintain the normal development of tapetum and pollen grains under adverse environmental conditions. Although we are still unclear at present about the transcript form of *LTT1*, the outstanding cold tolerance conferred by the mutation would greatly promote the sustainable development of rice in high-altitude regions.

ACKNOWLEDGMENTS

This work was supported by grants from the National Key Research and Development Program of China (Grant 2016YFD0101801) and the State Key Laboratory of Plant Genomics (SKLPG2011B0403). We thank Mr. Yanbao Tian (Institute of Genetics and Developmental Biology) for the help in scanning electron microscopy analysis.

ORCID

Yufang Xu https://orcid.org/0000-0002-3018-0722
Shanguo Yao https://orcid.org/0000-0001-9398-785X

REFERENCES

Avramova, Z. (2015). Transcriptional 'memory' of a stress: Transient chromatin and memory (epigenetic) marks at stress-response genes. *Plant Journal*, *83*(1), 149–159.

Baier, M., Bittner, A., Prescher, A., & van Buer, J. (2019). Preparing plants for improved cold tolerance by priming. *Plant, Cell and Environment*, *42*(3), 782–800.

Baxter, A., Mittler, R., & Suzuki, N. (2014). ROS as key players in plant stress signalling. *Journal of Experimental Botany*, *65*(5), 1229–1240.

Ben Rejeb, K., Lefebvre-De Vos, D., Le Disquet, I., Leprince, A.S., Bordenave, M., Maldiney, R., … Savoure, A. (2015). Hydrogen peroxide produced by NADPH oxidases increases proline accumulation during salt or mannitol stress in *Arabidopsis thaliana*. *New Phytologist*, *208*(4), 1138–1148.

Chen, H., Li, C., Liu, L., Zhao, J., Cheng, X., Jiang, G., & Zhai, W. (2016). The Fd-GOGAT1 mutant gene *lc7* confers resistance to *Xanthomonas oryzae* pv. *Oryzae* in rice. *Scientific Reports*, *6*, 26411.

Chen, Z. S., Liu, X. F., Wang, D. H., Chen, R., Zhang, X. L., Xu, Z. H., & Bai, S. N. (2018). Transcription factor OsTGA10 is a target of the MADS protein OsMADS8 and is required for tapetum development. *Plant Physiology*, *176*(1), 819–835.

Cheng, C., Yun, K. Y., Ressom, H. W., Mohanty, B., Bajic, V. B., Jia, Y., … de los Reyes, B. G. (2007). An early response regulatory cluster induced by low temperature and hydrogen peroxide in seedlings of chilling-tolerant japonica rice. *BMC Genomics*, *8*, 175.

Choudhury, F. K., Rivero, R. M., Blumwald, E., & Mittler, R. (2017). Reactive oxygen species, abiotic stress and stress combination. *Plant Journal*, *90*(5), 856–867.

Dreyer, A., & Dietz, K. J. (2018). Reactive oxygen species and the redox-regulatory network in cold stress acclimation. *Antioxidants*, *7*(11), 169.

Friedrich, T., Faivre, L., Bäurle, I., & Schubert, D. (2018). Chromatin-based mechanisms of temperature memory in plants. *Plant, Cell and Environment*, *42*(3), 762–770.

Fu, Z., Yu, J., Cheng, X., Zong, X., Xu, J., Chen, M., … Liang, W. (2014). The rice basic helix-loop-helix transcription factor TDR INTERACTING PROTEIN2 is a central switch in early anther development. *Plant Cell*, *26*(4), 1512–1524.

Fujino, K., Sekiguchi, H., Matsuda, Y., Sugimoto, K., Ono, K., & Yano, M. (2008). Molecular identification of a major quantitative trait locus, *qLTG3-1*, controlling low-temperature germinability in rice. *Proceedings of the National Academy of Sciences of the United States of America*, *105*(34), 12623–12628.

Garg, B., Jaiswal, J. P., Misra, S., Tripathi, B. N., & Prasad, M. (2012). A comprehensive study on dehydration-induced antioxidative responses during germination of Indian bread wheat (*Triticum aestivum* L. em Thell) cultivars collected from different agroclimatic zones. *Physiology and Molecular Biology of Plants*, *18*(3), 217–228.

Gross, B. L., & Zhao, Z. (2014). Archaeological and genetic insights into the origins of domesticated rice. *Proceedings of the National Academy of Sciences of the United States of America*, *111*(17), 6190–6197.

Hossain, M.A., Bhattacharjee, S., Armin, S.M., Qian, P., Xin, W., Li, H.Y., … Tran, L.S. (2015). Hydrogen peroxide priming modulates abiotic oxidative stress tolerance: Insights from ROS detoxification and scavenging. *Frontiers in Plant Science*, *6*, 420.

Hu, L., Liang, W., Yin, C., Cui, X., Zong, J., Wang, X., … Zhang, D. (2011). Rice MADS3 regulates ROS homeostasis during late anther development. *Plant Cell*, *23*(2), 515–533.

Ito, Y., Saisho, D., Nakazono, M., Tsutsumi, N., & Hirai, A. (1997). Transcript levels of tandem-arranged alternative oxidase genes in rice are increased by low temperature. *Gene*, *203*(2), 121–129.

Ji, C., Li, H., Chen, L., Xie, M., Wang, F., Chen, Y., & Liu, Y. G. (2013). A novel rice bHLH transcription factor, DTD, acts coordinately with TDR in controlling tapetum function and pollen development. *Molecular Plant*, *6*(5), 1715–1718.

Jung, K.H., Han, M.J., Lee, Y.S., Kim, Y.W., Hwang, I., Kim, M.J., … An, G. (2005). Rice *Undeveloped Tapetum1* is a major regulator of early tapetum development. *Plant Cell*, *17*(10), 2705–2722.

Kaur, G., Guruprasad, K., Temple, B. R. S., Shirvanyants, D. G., Dokholyan, N. V., & Pati, P. K. (2018). Structural complexity and functional diversity of plant NADPH oxidases. *Amino Acids*, *50*(1), 79–94.

Kim, S. H., Choi, H. S., Cho, Y. C., & Kim, S. R. (2011). Cold-responsive regulation of a flower-preferential class III peroxidase gene, *OsPOX1*, in rice (*Oryza sativa* L.). *Journal of Plant Biology*, *55*(2), 123–131.

Ko, S.S., Li, M.J., Lin, Y.J., Hsing, H.X., Yang, T.T., Chen, T.K., … Ku, M.S. (2017). Tightly controlled expression of *bHLH142* is essential for timely tapetal programmed cell death and pollen development in rice. *Frontiers in Plant Science*, *8*, 1258.

Ko, S.S., Li, M.J., Sun-Ben Ku, M., Ho, Y.C., Lin, Y.J., Chuang, M.H., … Chan, M.T. (2014). The bHLH142 transcription factor coordinates with TDR1 to modulate the expression of *EAT1* and regulate pollen development in rice. *Plant Cell*, *26*(6), 2486–2504.

Lee, S. C., Kwon, S. Y., & Kim, S. R. (2009). Ectopic expression of a cold-responsive CuZn superoxide dismutase gene, *SodCc1*, in transgenic rice (*Oryza sativa* L.). *Journal of Plant Biology*, *52*(2), 154–160.

Li, C. R., Liang, D. D., Xu, R. F., Li, H., Zhang, Y. P., Qin, R. Y., … Yang, J. B. (2013). Overexpression of an alternative oxidase gene, *OsAOX1a*, improves cold tolerance in *Oryza sativa* L. *Genetics and Molecular Research*, *12*(4), 5424–5432.

Li, H., Yuan, Z., Vizcay-Barrena, G., Yang, C., Liang, W., Zong, J., … Zhang, D. (2011). *PERSISTENT TAPETAL CELL1* encodes a PHD-finger protein that is required for tapetal cell death and pollen development in rice. *Plant Physiology*, *156*(2), 615–630.

Li, N., Zhang, D. S., Liu, H. S., Yin, C. S., Li, X. X., Liang, W. Q., … Zhang, D. B. (2006). The rice tapetum degeneration retardation gene is required for tapetum degradation and anther development. *Plant Cell*, *18*(11), 2999–3014.

Li, S., Castillo-Gonzalez, C., Yu, B., & Zhang, X. (2017). The functions of plant small RNAs in development and in stress responses. *Plant Journal*, *90*(4), 654–670.

Liu, C., Ou, S., Mao, B., Tang, J., Wang, W., Wang, H., … Chu, C. (2018). Early selection of *bZIP73* facilitated adaptation of *japonica* rice to cold climates. *Nature Communications*, *9*(1), 3302.

Liu, C., Schlappi, M. R., Mao, B., Wang, W., Wang, A., & Chu, C. (2019). The bZIP73 transcription factor controls rice cold tolerance at the reproductive stage. *Plant Biotechnology Journal*, *17*(9), 1834–1849.

Lu, G., Wu, F. Q., Wu, W., Wang, H. J., Zheng, X. M., Zhang, Y., … Wan, J. (2014). Rice *LTG1* is involved in adaptive growth and fitness under low ambient temperature. *Plant Journal*, *78*(3), 468–480.

Luo, D., Xu, H., Liu, Z., Guo, J., Li, H., Chen, L., … Liu, Y. G. (2013). A detrimental mitochondrial-nuclear interaction causes cytoplasmic male sterility in rice. *Nature Genetics*, *45*(5), 573–577.

Ma, Y., Dai, X., Xu, Y., Luo, W., Zheng, X., Zeng, D., … Chong, K. (2015). *COLD1* confers chilling tolerance in rice. *Cell*, *160*(6), 1209–1221.

Mao, D., Xin, Y., Tan, Y., Hu, X., Bai, J., Liu, Z. Y., … Chen, C. (2019). Natural variation in the *HAN1* gene confers chilling tolerance in rice and allowed adaptation to a temperate climate. *Proceedings of the National Academy of Sciences of the United States of America*, *116*(9), 3494–3501.

Marino, D., Dunand, C., Puppo, A., & Pauly, N. (2012). A burst of plant NADPH oxidases. *Trends in Plant Science*, *17*(1), 9–15.

Mittler, R. (2017). ROS are good. *Trends in Plant Science*, *22*(1), 11–19.

Niu, N., Liang, W., Yang, X., Jin, W., Wilson, Z. A., Hu, J., & Zhang, D. (2013). EAT1 promotes tapetal cell death by regulating aspartic proteases during male reproductive development in rice. *Nature Communications*, *4*, 1445.

Ouyang, S. Q., Liu, Y. F., Liu, P., Lei, G., He, S. J., Ma, B., … Chen, S. Y. (2010). Receptor-like kinase OsSIK1 improves drought and salt stress tolerance in rice (*Oryza sativa*) plants. *Plant Journal*, *62*(2), 316–329.

Peres, M. D. G., Basu, S., Ramegowda, V., Braga, E. B., & Pereira, A. (2016). Comparative analysis of gene expression in response to cold stress in diverse rice genotypes. *Biochemical and Biophysical Research Communications*, *471*(1), 253–259.

Phan, H. A., Li, S. F., & Parish, R. W. (2012). MYB80, a regulator of tapetal and pollen development, is functionally conserved in crops. *Plant Molecular Biology*, *78*(1–2), 171–183.

Saito, K., Hayano-Saito, Y., Kuroki, M., & Sato, Y. (2010). Map-based cloning of the rice cold tolerance gene *Ctb1*. *Plant Science*, *179*(1–2), 97–102.

Sakamoto, T., Morinaka, Y., Ohnishi, T., Sunohara, H., Fujioka, S., Ueguchi-Tanaka, M., … Matsuoka, M. (2006). Erect leaves caused by brassinosteroid deficiency increase biomass production and grain yield in rice. *Nature Biotechnology*, *24*(1), 105–109.

Sato, Y., Masuta, Y., Saito, K., Murayama, S., & Ozawa, K. (2011). Enhanced chilling tolerance at the booting stage in rice by transgenic overexpression of the ascorbate peroxidase gene, *OsAPXa*. *Plant Cell Reports*, *30*(3), 399–406.

Sharma, K. D., & Nayyar, H. (2016). Regulatory networks in pollen development under cold stress. *Frontiers in Plant Science*, *7*, 402.

Shi, W., Li, X., Schmidt, R. C., Struik, P. C., Yin, X., & Jagadish, S. V. K. (2018). Pollen germination and in vivo fertilization in response to high-temperature during flowering in hybrid and inbred rice. *Plant, Cell and Environment*, *41*(6), 1287–1297.

Suzuki, K., Aoki, N., Matsumura, H., Okamura, M., Ohsugi, R., & Shimono, H. (2015). Cooling water before panicle initiation increases chilling-induced male sterility and disables chilling-induced expression of genes encoding OsFKBP65 and heat shock proteins in rice spikelets. *Plant, Cell and Environment*, *38*(7), 1255–1274.

Suzuki, N., Miller, G., Morales, J., Shulaev, V., Torres, M. A., & Mittler, R. (2011). Respiratory burst oxidases: The engines of ROS signaling. *Current Opinion in Plant Biology*, *14*(6), 691–699.

Tao, Z., Kou, Y., Liu, H., Li, X., Xiao, J., & Wang, S. (2011). *OsWRKY45* alleles play different roles in abscisic acid signalling and salt stress tolerance but similar roles in drought and cold tolerance in rice. *Journal of Experimental Botany*, *62*(14), 4863–4874.

Tovuu, A., Zulfugarov, I. S., Wu, G., Kang, I. S., Kim, C., Moon, B. Y., … Lee, C. H. (2016). Rice mutants deficient in ω-3 fatty acid desaturase (FAD8) fail to acclimate to cold temperatures. *Plant Physiology and Biochemistry*, *109*, 525–535.

Wang, J., Meng, X., Dobrovolskaya, O. B., Orlov, Y. L., & Chen, M. (2017a). Non-coding RNAs and their roles in stress response in plants. *Genomics, Proteomics & Bioinformatics*, *15*(5), 301–312.

Wang, J., Wang, R., Wang, Y., Zhang, L., Zhang, L., Xu, Y., & Yao, S. (2017b). *Short and Solid Culm/RFL/APO2* for culm development in rice. *Plant Journal*, *91*(1), 85–96.

Wu, W., Zheng, X. M., Lu, G., Zhong, Z., Gao, H., Chen, L., … Wan, J. (2013). Association of functional nucleotide polymorphisms at *DTH2* with the northward expansion of rice cultivation in Asia. *Proceedings of the National Academy of Sciences of the United States of America*, *110*(8), 2775–2780.

Xiao, N., Gao, Y., Qian, H., Gao, Q., Wu, Y., Zhang, D., … Li, A. (2018). Identification of genes related to cold tolerance and a functional allele that confers cold tolerance. *Plant Physiology*, *177*(3), 1108–1123.

Xie, G., Kato, H., & Imai, R. (2012). Biochemical identification of the OsMKK6-OsMPK3 signalling pathway for chilling stress tolerance in rice. *Biochemical Journal*, *443*(1), 95–102.

Xie, H. T., Wan, Z. Y., Li, S., & Zhang, Y. (2014). Spatiotemporal production of reactive oxygen species by NADPH oxidase is critical for tapetal programmed cell death and pollen development in *Arabidopsis*. *Plant Cell*, *26*(5), 2007–2023.

Xue, W., Xing, Y., Weng, X., Zhao, Y., Tang, W., Wang, L., … Zhang, Q. (2008). Natural variation in *Ghd7* is an important regulator of heading date and yield potential in rice. *Nature Genetics*, *40*(6), 761–767.

Yang, L., Qian, X., Chen, M., Fei, Q., Meyers, B. C., Liang, W., & Zhang, D. (2016). Regulatory role of a receptor-like kinase in specifying anther cell identity. *Plant Physiology*, *171*(3), 2085–2100.

Ye, N., Zhu, G., Liu, Y., Li, Y., & Zhang, J. (2011). ABA controls H_2O_2 accumulation through the induction of *OsCATB* in rice leaves under water stress. *Plant and Cell Physiology*, *52*(4), 689–698.

Yi, J., Moon, S., Lee, Y. S., Zhu, L., Liang, W., Zhang, D., … An, G. (2016). Defective tapetum cell death 1 (DTC1) regulates ROS levels by binding to metallothionein during tapetum degeneration. *Plant Physiology*, *170*(3), 1611–1623.

Yu, S. X., Feng, Q. N., Xie, H. T., Li, S., & Zhang, Y. (2017). Reactive oxygen species mediate tapetal programmed cell death in tobacco and tomato. *BMC Plant Biology*, *17*(1), 76.

Zhang, D., Luo, X., & Zhu, L. (2011). Cytological analysis and genetic control of rice anther development. *Journal of Genetics and Genomics*, *38*(9), 379–390.

Zhang, D. S., Liang, W. Q., Yuan, Z., Li, N., Shi, J., Wang, J., … Zhang, D. B. (2008). Tapetum degeneration retardation is critical for aliphatic metabolism and gene regulation during rice pollen development. *Molecular Plant*, *1*(4), 599–610.

Zhang, J., Luo, W., Zhao, Y., Xu, Y., Song, S., & Chong, K. (2016). Comparative metabolomic analysis reveals a reactive oxygen species-dominated dynamic model underlying chilling environment adaptation and tolerance in rice. *New Phytologist*, *211*(4), 1295–1310.

Zhang, Q., Chen, Q., Wang, S., Hong, Y., & Wang, Z. (2014). Rice and cold stress: Methods for its evaluation and summary of cold tolerance-related quantitative trait loci. *Rice*, *7*(1), 24.

Zhang, Z., Li, J., Pan, Y., Li, J., Zhou, L., Shi, H., … Li, Z. (2017). Natural variation in *CTB4a* enhances rice adaptation to cold habitats. *Nature Communications*, *8*, 14788.

Zheng, S., Li, J., Ma, L., Wang, H., Zhou, H., Ni, E., … Zhuang, C. (2019). OsAGO2 controls ROS production and the initiation of tapetal PCD by epigenetically regulating *OsHXK1* expression in rice anthers. *Proceedings of the National Academy of Sciences of the United States of America*, *116*(15), 7549–7558.

SUPPORTING INFORMATION

Additional supporting information may be found online in the Supporting Information section at the end of this article.

How to cite this article: Xu Y, Wang R, Wang Y, Zhang L, Yao S. A point mutation in *LTT1* enhances cold tolerance at the booting stage in rice. *Plant Cell Environ*. 2020;43:992–1007. https://doi.org/10.1111/pce.13717